Bilateral NIST-PTB Comparison of Spectral Responsivity in the VUV

A Gottwald[1], M Richter[1], P-S Shaw[2], Z Li[2] and U Arp[2]

[1]Physikalisch-Technische Bundesanstalt, Abbestraße 2-12, 10587 Berlin, Germany
[2]National Institute for Standards and Technology, 100 Bureau Dr., Gaithersburg, MD 20899-8410, U.S.A.

E-mail: alexander.gottwald@ptb.de

Abstract. To compare the calibration capabilities for the spectral responsivity in the vacuum-ultraviolet spectral region between 135 nm and 250 nm, PTB and NIST agreed on a bilateral comparison. Calibrations of semiconductor photodiodes as transfer detectors were performed using monochromatized synchrotron radiation and cryogenic electrical substitution radiometers as primary detector standards. Great importance was attached to the selection of suitable transfer detector standards due to their critical issues in that wavelength regime. The uncertainty budgets were evaluated in detail. The comparison showed a reasonable agreement between the participants. However, it got obvious that the uncertainty level for this comparison cannot easily be further reduced due to the lack of sufficiently radiation-hard and long-term stable transfer standard detectors.

1. Introduction

The last decade has seen numerous key comparisons in the field of photometry and radiometry between different national metrology institutes (NMIs) in the context of the Mutual Recognition Arrangement. At first, these comparisons were restricted to wavelengths longer than 200 nm, with just the exception of a recent pilot comparison from 10 nm to 20 nm [1]. There are multiple reasons for this: The request for calibration techniques and certificates for wavelengths below 200 nm is limited to a small, but growing number of applications and research fields. Moreover, at shorter wavelengths, the practical problems of accurate measurements, i. e. source and detector stabilities, become an increasing challenge. As a result, only a few NMIs have calibration capabilities in the spectral regimes of the vacuum-ultraviolet (VUV), extreme ultraviolet (EUV) and, moreover, in the subsequent shorter wavelengths of the soft X-ray region. However, in these spectral regimes, the steadily growing interest in radiometric calibrations is driven by industries (*e.g.* photolithography) and research fields such as extraterrestrial solar astronomy.

Due to the lack of stable, tunable laboratory radiation sources in the VUV, the use of monochromatized synchrotron radiation (SR) is essential, though not widely available. While electrical substitution radiometers (ESRs) are well-established as primary detector standards in the optical regime, their operation in the VUV with the specific characteristics of SR is somehow more critical [2,3]. Using SR of the storage rings SURF III (NIST) [4] and BESSY II (PTB) [5,6], both facilities offer regular calibration services for radiation detector devices with traceability to ESRs as primary standards. To validate the individual scales of spectral responsivity, we agreed to a bilateral comparison for the spectral region between 135 nm and 250 nm. A set of selected detectors had been calibrated by both participants, with PTB acting as pilot laboratory.

2. Measurement methods and capabilities

The different measurement facilities at PTB and NIST are described in the following subsections. For all measurements, the photodiodes were used in photovoltaic mode, i.e., the photocurrent was measured without the application of a bias voltage. In the VUV spectral range, the photon energy is sufficient to create photoelectrons by the external photoelectric effect. Therefore, in all cases the current must be measured from the substrate electrode of the diode, while the front side is kept on ground potential. Table 1 gives a compilation of the measurement conditions at both laboratories.

2.1 PTB facilities

The measurements at PTB were performed using monochromatized SR from the UV- and VUV beamline for detector calibration located at the PTB laboratory at the electron storage ring BESSY II [7]. A cryogenic electrical substitution radiometer was used as the primary detector standard. Using five different beamlines and two different cryogenic radiometers, PTB maintains and disseminates a scale of spectral responsivity from 400 nm (3 eV) to 0.02 nm (60 keV) [3,8]. The beamlines are carefully characterized concerning their spectral purity, because of the impact of spectral false light on the measurement uncertainty. At the UV/VUV beamline, different bulk filters allow the suppressing of unwanted spectral orders from the monochromator, *e.g.* an MgF_2 filter for the 120 nm to 180 nm spectral range and a quartz filter between 180 nm and 250 nm. The 1-m normal incidence monochromator (NIM) is used with a 600 lines/mm aluminium-coated grating, which gives a spectral bandwith of 0.9 nm and typical spectral radiant powers between approximately 100 nW at 120 nm and 1 μW at 250 nm, depending on the electron current stored in the storage ring. The typical spot size on the detector is about 1 mm vertical and 3 mm horizontal. For spatial mapping of the detector uniformity, the spot size was reduced by an aperture down to approximately 1 mm in diameter. The cryogenic radiometer SYRES II (SYnchrotron Radiation Electrical Substitution radiometer) [9] is designed to bring the absorbing cavity and the detector to be calibrated in the same position relative to the radiation beam, consecutively. During measurements, the intensity of the radiation is monitored

using a beamsplitter system, which decouples a few percent of the radiant power. The temperature of the detector to be calibrated is controlled and stabilized to 25 °C using Peltier heating/cooling.

The uncertainty budget for a detector calibration is exemplified in table 2 for a wavelength of 193 nm. It is dominated, on the one hand, by the contribution from the radiant power determination using the radiometer. On the other hand, the out-of-band contribution to the calibration is the second important source of uncertainty, despite the efforts to minimize its effects by filtering.

2.2 NIST facilities

Similar to the PTB measurements, the NIST set-up employed monochromatic SR provided by the 2-m normal incidence monochromator at beamline 4 at the Synchrotron Ultraviolet Radiation Facility (SURF III) [2]. A cryogenic radiometer was used as the primary detector standard [10]. Beamline 4 calibrations covered the ultraviolet spectral range from 130 nm to 320 nm. The ultrahigh vacuum of the monochromator is separated from the beamline end-station by a CaF_2 window, which greatly reduces turnaround time when detectors under test are changed and also doubles as an order-sorting filter between 130 nm and 200 nm. To suppress higher order reflections of the grating, a quartz window is translated into the beam exiting the monochromator at wavelengths longer than 200 nm. Using a 600 line/mm grating and an exit slit opening of 2 mm × 2 mm the spectral bandwidth was approximately 1.4 nm at 200 nm wavelength. The exit slit is imaged onto the detector resulting into an illuminated area of 2 mm × 2 mm. The output power of the beamline had a maximum of approximately 1 µW at 200 nm wavelength and falls to about 200 nW at 130 nm and 320 nm. Just before the detector under test a cryogenic radiometer a CaF_2 beamsplitter is used to reflect part of the incoming radiation onto a photodiode in order to monitor the actual intensity, which decreases over time because of the limited lifetime of the electron beam stored in the storage ring. The wavelength calibration of the beamline was established using a holmium solution wavelength standard (NIST SRM 2034) [2]. The uncertainty budget (exemplified for a wavelength of 135 nm) is shown in table 3.

3. Relevant characteristics and selection of the detectors

Typically, semiconductor photodiodes are used as secondary standards which can be calibrated against the primary standard with uncertainties below 1 %. At this level of uncertainty, the detector characteristics play a non-negligible role in the uncertainty budget. Usually, the homogeneity (or spatial uniformity) and the radiation hardness of the detector are critical issues. In the long-term use of a detector standard, its stability (concerning degradation) is the limiting factor. For the comparison, a set of detectors was chosen (see table 4), which had already been proved to be suitable candidates as transfer standards in this spectral range. There were three different diode types: First, the AXUV-100G is a silicon p-n junction photodiode without a doped dead-region which only has a thin (few nm) silicon oxide layer on the surface. These diodes are commonly used for radiometric purposes [11]. However, they are known to show significant degradation when exposed to VUV or EUV radiation [12,13,14]. The second diode type we used, the SXUV-100, is basically the same as the AXUV with a metallic surface layer to reduce radiation damage. The third type of diode is the SUV 100, a Schottky-type PtSi-nSi photodiode, which has proved to be highly stable when exposed to VUV irradiation [13,15]. The comparison was limited to these three detector types for practical reasons, although there are more detectors which could in principle be used for this.

The selected detectors were tested in the comparison's wavelength interval for their critical characteristics, *i.e.* spatial uniformity, stability, temperature behaviour, and linearity. Some of test measurements were extended down to 120 nm to cover the hydrogen Lyman-α wavelength of 121.6 nm. At first glance, the three detectors differed in their absolute spectral responsivity by an order of magnitude (figure 1): Due to their metallic top layers, SXUV-100 and SUV 100 only showed values of about $0.01\,\mathrm{AW}^{-1}$ in the wavelength region between 120 nm and 250 nm, whereas the AXUV-100G had more than ten times higher responsivity.

3.1 Temperature coefficient

The absolute responsivity of semiconductor photodiodes depends on the device temperature [16]. To be able to correct for different detector temperatures, the change of the spectral responsivity with the temperature (relative to the value at 20 °C) was determined. For the different detectors, calibrations were performed in a ±5 K temperature interval. Figure 2 depicts the average relative change in spectral responsivity for this temperature interval. It is generally small (less than 0.1 % for a 1 K change in temperature), with the SUV 100 (Schottky-type) diode having the largest value. Moreover, the SUV 100 is the only detector showing a significant change of the temperature coefficient with a wavelength in the investigated range. Regarding the uncertainties, it should be noted that these are only the reproducibility uncertainties (k=1) which are naturally much smaller than the total uncertainties in the absolute determination of spectral responsivity.

3.2 Linearity

The linearity in the spectral responsivity of semiconductor photodiodes is limited by saturation effects which occur at high radiation intensities. Although usually calibrations using monochromatized SR are performed at low intensities, we investigated the deviations from linearity. To do so, we calibrated the detectors at different levels of radiant power at a wavelength of 193 nm. This was realized using the high dynamics in radiant power from a storage ring by changing the stored electron beam current. For radiant powers below 1 µW, the results in figure 3 show that the responsivity stays linear for all three types of detectors within the limits of experimental uncertainty, and no non-linearity corrections need to be applied.

3.3 Spatial uniformity

To test the detectors' spatial uniformity in their spectral responsivities, the detectors were scanned over the whole active surface area with a 1-mm diameter beam while recording their signal current. This was done at the three wavelengths of 121.6 nm (Lyman-α), 157 nm, and 193 nm; the latter two corresponding to excimer laser wavelengths. Figure 4(a) shows an example of a relative responsivity

map for an AXUV-100G photodiode at 193 nm. From these measurements, the relative change in responsivity with changing beam size was calculated under the assumption of a homogeneous radiation beam, to estimate the resulting uncertainty contribution from the detector non-uniformities. The result is given in table 5 for a change of beam size from 3 mm × 1 mm (as for the PTB calibrations) to square beams of 2 mm × 2 mm and 4 mm × 4 mm, respectively, calculated for a virtual spot in the centre of the detector. Since the real beam profiles at the respective SR beamlines are not known with sufficient accuracy, it is not possible to correct the results, but only to account for this in the uncertainty budget. The resulting change, *e.g.* is only a fraction of a percent for the AXUV-100G at 193 nm, however, the non-uniformity rises towards shorter wavelengths.

3.4 Irradiation stability

The radiation stability of the different detectors was determined as the relative difference of the spectral responsivity before and after irradiation with monochromatized synchrotron radiation at 193 nm (2 mJ total radiant exposure) and 121.6 nm (0.6 mJ total radiant exposure). Hence, spatial uniformity maps of the detectors were recorded at both wavelengths before and after irradiation. These relatively high exposures (in comparison to typical calibration measurements) were realized by long-time (approximately 1 h) irradiations. Figure 4(b) gives an example of the relative difference in responsivity of the AXUV-100G photodiode at 121 nm after irradiation at the same wavelength. The irradiance spot can clearly be seen. Table 6 summarizes the measurement results. Here, again, the relative change in responsivity was calculated from the difference map for a beam size of 3 mm × 1 mm. In some cases, where the change was small, only an upper limit for the change was deduced. This was mainly the case where the irradiation spot could not be identified from the non-uniformity or in the reproducibility of the two measurements. The result shows, that all detectors remain stable at 193 nm after irradiation at the same wavelength. At 121.6 nm, only the SUV 100 shows significant degradation after the 193 nm irradiation. The situation is different for the 121.6 nm irradiation: Here, all detectors except for the SUV 100 show degradation also at the long wavelength (193 nm), and

strong degradation at the irradiation wavelength of 121.6 nm. Moreover, the AXUV/SXUV type diodes which seem to have higher stability against 193 nm irradiation, show stronger degradation at 121.6 nm than the SUV diode. The results show that all detectors in the comparison are subject to damage by radiation, and therefore, must be checked for their spatial uniformity before and after the calibrations, so that irradiation damage (as it is spatially discrete) can be detected and considered in data evaluation.

Generally, the measurements show that none of the detectors can be regarded as ideally suited over the complete wavelength range of the comparison. Each has its specific strengths and weaknesses, so it seems to be appropriate to use several detectors in a mix.

4. Realization of the comparison

For the comparison, a total of four detectors were used (see table 4). The first (initial) calibration at PTB took place in October 2006, the NIST calibration in May 2007, and the final re-calibration at PTB in August 2007. The detectors were calibrated at NIST and PTB facilities using standard calibration routines. A set of two reference detectors was stored at PTB under dry air without being exposed to radiation, to be able to recognize systematic changes, *e.g.* through the transport.

Figure 5 gives an overview of the long-term stability of the transfer standards. Here, the relative difference in the absolute spectral responsivity versus wavelength is shown for the initial and final calibrations at PTB. For the AXUV-100G and SXUV-100, the index "A" marks the detectors used for the comparison, while the detectors marked "B" were kept as reference detectors. Unfortunately, the SXUV "A" detector underwent a change in responsivity of more than 10 % during the (first) transport from PTB to NIST due to unknown reasons, resulting in a complete mismatch between the two measurements at PTB. Therefore, it is not shown in this figure. However, since there was a reasonable match between the NIST and final PTB calibration data, it was still used for comparison. For all detectors, spatial uniformity maps were recorded at 193 nm and 121.6 nm, before initial and after final calibration. None of the detectors showed a distinct degradation which could be assigned to radiation

damage, so that no correction for degradation (according to section 3.4) was applied to the data. Regarding figure 5, the detectors show no uniform behaviour in ageing; neither the different types nor the different individuals of the same type. While, *e.g.*, one of the AXUV "A" detectors almost remains constant at better than 0.3 % over the complete spectral range, the other specimen changes more than 1 % with significant wavelength dependent behaviour, particularly a strong decrease below 160 nm wavelength. The reference detectors "B" both only show a small change, *i.e.* less than a 0.5 % decrease in responsivity.

These results show the limits in long-term stability in which the results of the comparison must be interpreted. In particular in the short wavelength limit of the comparison, *i.e.* below 160 nm, the detectors tend to have an increased change in responsivity with time and/or irradiation.

5. Results and discussion

The result of the comparison is concluded in figure 6. It shows the relative deviation of the calibrations from the median, averaged over the four detectors used in the comparison. To obtain the deviation, the data were analyzed as follows: For each detector, at each wavelength measured, the weighted mean (with the extended uncertainty $k=2$ of the individual measurement as weight) between the PTB and the NIST measurement was taken, and the deviation of each measurement from this median was calculated. For the four different detectors, the weighted mean of these deviations was taken, with the resulting uncertainty as the combined uncertainties from the individual detectors. It should be noticed that the shown uncertainties do not include any contribution from the detector long-term stability. To account for this contribution, the same procedure to calculate the median was applied to the results from the long-term stability measurements described in section 4 (see figure 5): The values given by the lines in figure 6 are calculated as the mean absolute deviation between initial and final calibration at PTB, averaged overall detectors used in the comparison (set "A"). These values might be regarded as additional uncertainty contribution, and were shown in figure 6 as solid line. Although the deviations are different for the individual detectors, we believe that this gives an

overall indication for the range of detector stability which can be expected. To include this stability term, an additional uncertainty (given by the lines in figure 6) must be added to the uncertainties arising from the calibrations itself (given by the error bars). Then, within the limits defined by the detector stability, one sees that there is an agreement between the NIST and the PTB calibrations within the extended uncertainties (k=2). In general, the NIST calibrations deliver slightly higher values for the spectral responsivity than PTB, which results in a positive value for the deviation. The lower total uncertainty of the PTB calibration leads to a higher weight in the averaging, i.e. a smaller deviation from the median. Towards shorter wavelengths, below 160 nm, there is some tendency for the values to diverge. However, this cannot be regarded as significant within the stability and uncertainty limits. The level of uncertainty in measurement, in particular for the PTB calibrations, corresponds to the level of stability of the detectors over the one-year re-calibration cycle, so that no further improvement can be reached without increasing the detector stability first. Although the detectors showed differences in their stability, none of the detector types used revealed superior behaviour, *i.e.* the characteristics seem to depend strongly on the individual detector used.

In summary, PTB and NIST performed a comparison of spectral responsivity measurements in the 135 nm to 250 nm spectral range. Both participants used monochromatized SR and a cryogenic radiometer as the primary standard detector, and realized the measurements with comparable levels of uncertainty. The uncertainty contributions from just the measurements showed to be of the same magnitude than those from detector used as transfer standards, particularly the stability of available photodiodes. This result is similar to the EUV comparison recently published [1], so that future work should be focussed on the search for more stable reference detectors.

Tables

Table 1. Compilation of the measurement conditions at the participating laboratories

	PTB	**NIST**
Spectral band width	0.9 nm	1.4 nm
Beam spot size	1mm x 3 mm	2 mm x 2mm
Beam divergence	12 mrad	20 mrad
Diode temperature	25 °C	22 °C
Typical radiant power	100 nW to 1 µW	200 nW to 1 µW
Current measurement	short circuit	short circuit
Polarity	surface grounded	surface grounded

Table 2. Compilation of the contributions to the uncertainty budget for the determination of the

spectral responsivity of a photodetector at PTB, using the cryogenic radiometer SYRES II and

monochromatized synchrotron radiation. The values are determined for a Si photodiode at a

wavelength of 193 nm, and are subject to change with the individual detector properties.

Quantity	Term	Relative extended uncertainty contribution (k=2) / %
Directly measured quantities:		
Measured photocurrent	$I_{\mathrm{P,i}}(\lambda)$	0.06
Dark current	$I_{\mathrm{D,i}}$	0.006
Normalization (monitor) current	$I_{\mathrm{M,i}}(\lambda)$	0.18
Normalized radiant power	$\Phi(\lambda)/I_{\mathrm{M}}(\lambda)$	0.40
Corrections for:		
Out-of-band stray light	$K_{\mathrm{FL}}(\lambda)$	0.30
Wavelength deviation	$K_{\mathrm{WL}}(\lambda)$	0.04
Spectral bandwith	$K_{\mathrm{BP}}(\lambda)$	0.02
Temperature coefficient	$K_{\mathrm{T}}(\lambda)$	0.02
Detector inhomogeneity	K_{Homo}	0.02
Polarization dependency	$K_{\mathrm{Pol}}(\lambda)$	0.10
Detector non-linearity	$K_{\mathrm{NL}}(\lambda)$	0.12
Spectral responsivity	$s_{\lambda}(\lambda)$	**0.56**

Table 3. Compilation of the contributions to the uncertainty budget for the determination of the spectral responsivity of a photodetector at NIST, using the cryogenic radiometer ACR and monochromatized synchrotron radiation. The values are determined for a Si photodiode at a wavelength of 135 nm, and are subject to change with the individual detector properties.

Quantity	Term	Relative extended uncertainty contribution (k=2) / %
ACR power measurement at 200 nW	$P_{ACR}(\lambda)$	0.70
Monitor diode current measurement	$I_M(\lambda)$	0.10
Test diode current measurements	$I_{DUT}(\lambda)$	0.10
Wavelength scale and spectral bandwidth	$K_{Mono}(\lambda)$	0.3
Test diode position	K_{Pos}	0.2
Out-of-band stray light	$K_{OOB}(\lambda)$	0.1
Spectral responsivity	$s_\lambda(\lambda)$	**0.81**

Table 4. List of detectors used for the comparison (comp.) and stored as reference at PTB (ref.).

| Detector name	Manufacturer	Type	Quantity (comp./ref.)
AXUV-100G	IRD Inc.	Si p-n	2/1
SXUV-100	IRD Inc.	Si p-n with TiN window	1/1
SUV 100	ETH Zürich/ SUV Detectors	PtSi-nSi Schottky	1/0

Table 5. Calculated change in responsivity with beam size changing from 3 mm × 1 mm (horizontal × vertical; beamsize at PTB) to 2 mm × 2 mm and 4 mm × 4 mm due to detector spatial non-uniformities. The calculation assumes a homogeneous radiation spot.

| Detector	Wavelength / nm	Rel. change in responsivity / % for beam size of	
		2 mm	**4 mm**
SUV 100	193	0.17	0.21
	157	0.18	0.21
	121.6	0.28	0.21
AXUV-100G	193	-0.01	0.12
	157	-0.01	0.12
	121.6	-0.14	-0.31
SXUV-100	193	-0.02	< -0.01
	157	-0.12	-0.08
	121.6	0.42	0.52

Table 6. Radiation stability of the detector types used for comparison.

| Irradiation wavelength / nm	Responsivity scan wavelength / nm	Max. rel. change in responsivity / %		
		SUV 100	**AXUV-100G**	**SXUV-100**
193				
	193	<0.1	<0.3	<0.1
	121.6	-1.4	<0.2	<0.3
121.6				
	193	<0.1	1.1	0.8
	121.6	-1.7	-6.6	-3.6

Figures
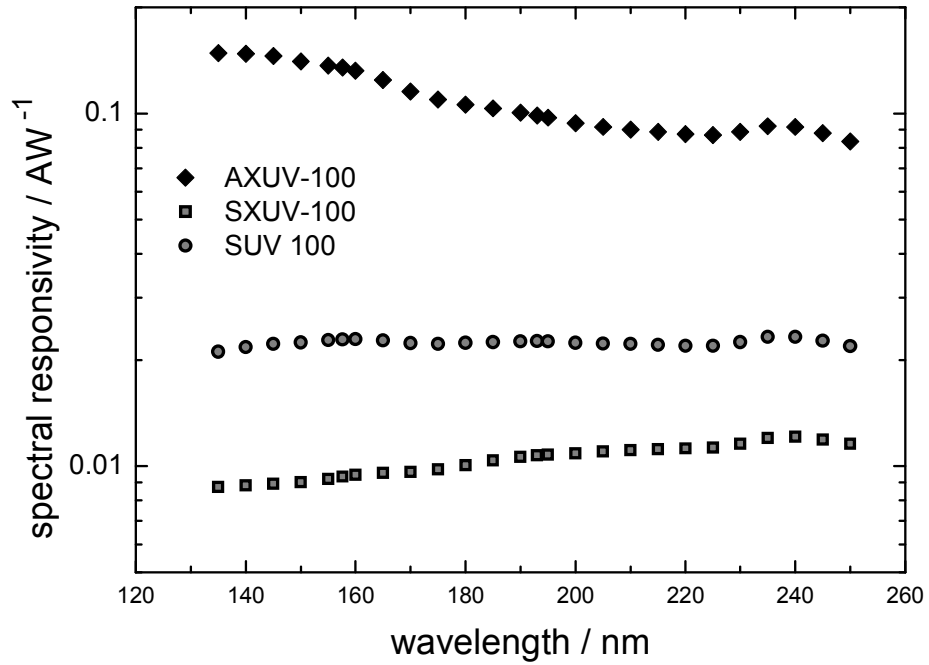
Figure 1. Overview of the spectral responsivity in the 135 nm to 250 nm wavelength region of the different types of detector used in the comparison (circles: SUV 100, squares: SXUV-100, diamonds: AXUV-100G).
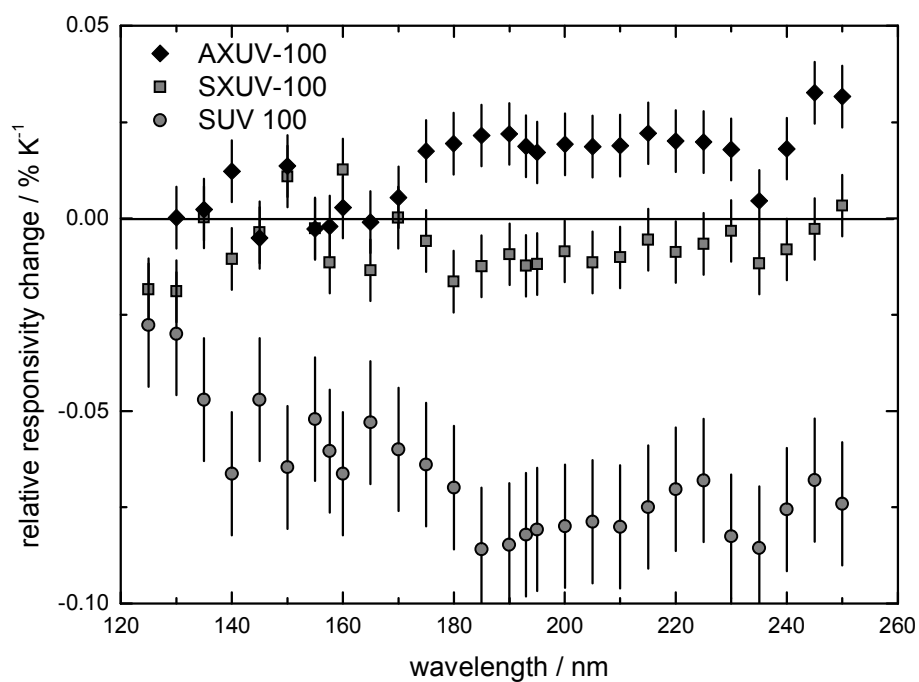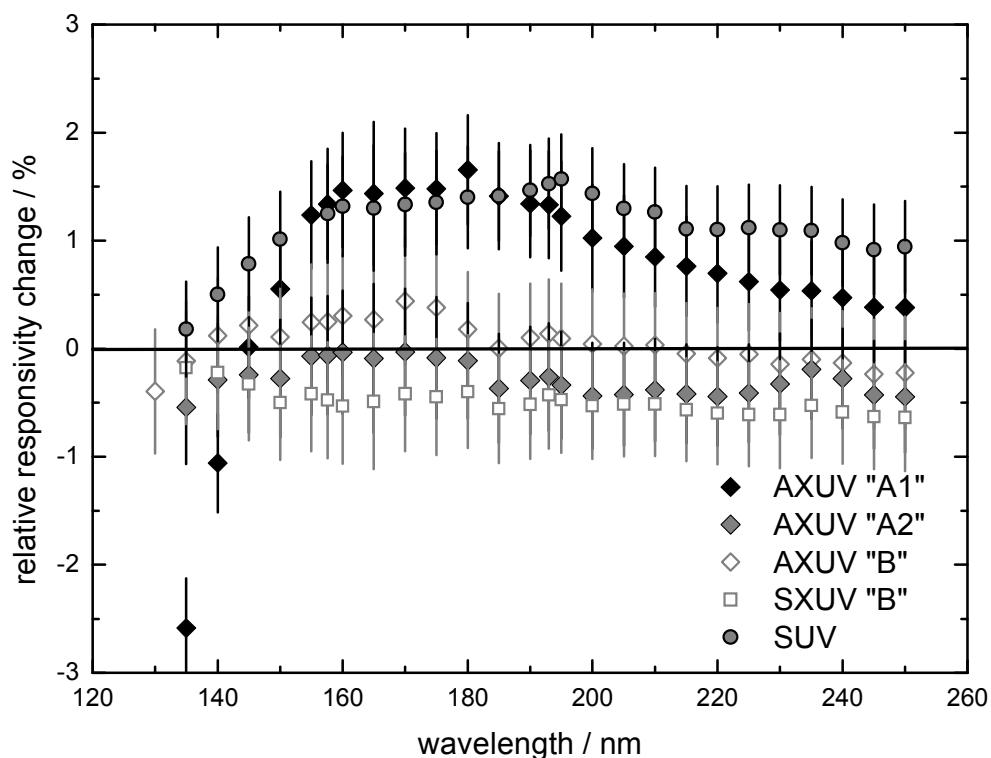
Figure 2. Temperature dependence of the spectral responsivity of the different types of detector used in the comparison (circles: SUV 100, squares: SXUV-100, diamonds: AXUV-100G). The relative change is the average measured at 20 °C for a +/- 5 °C interval.
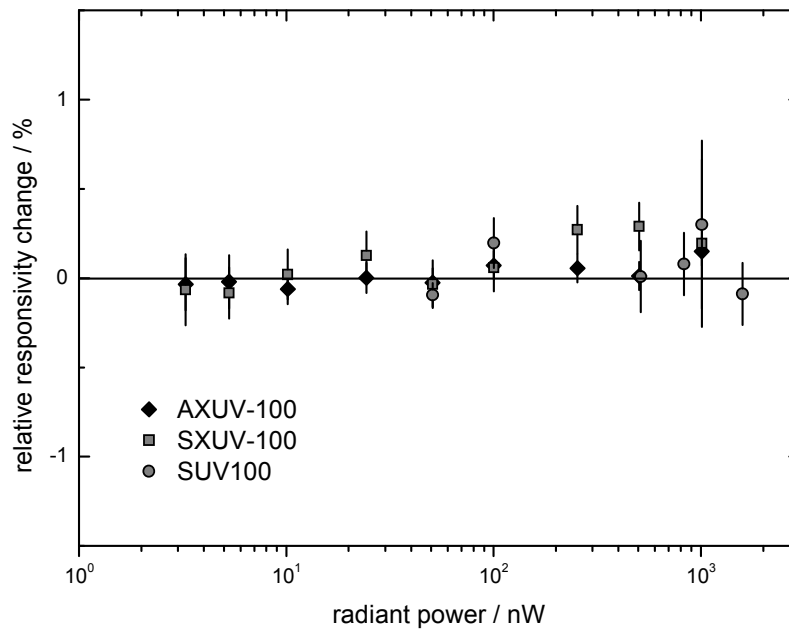
Figure 3. Linearity of the different types of detector used in the comparison (circles: SUV 100, squares: SXUV-100, diamonds: AXUV-100G). Shown is the relative change in responsivity at 193 nm for radiant powers between 3 nW and 1.01 μW. The zero line is given by the average for all values with radiant powers lower than 100 nW.
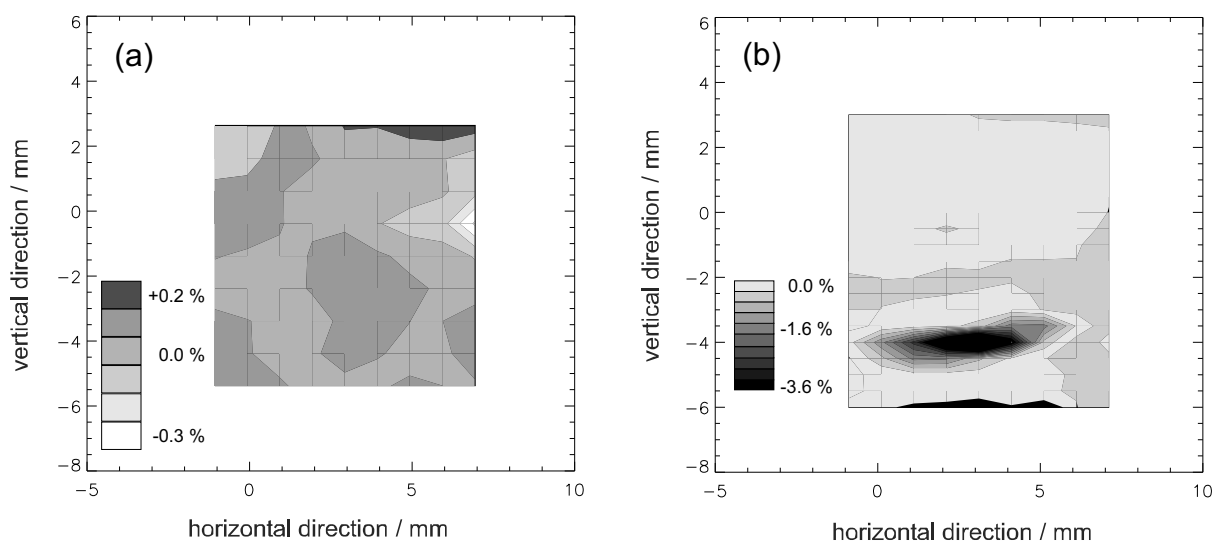
Figure 4. Example of spatial uniformity measurements. (a) Homogeneity: relative responsivity of an AXUV-100G photodetector at 193 nm. Each grey scale step corresponds to a 0.1 % change in responsivity. (b) Radiation stability: relative change in responsivity of an AXUV-100G photodetector at 121.6 nm after 0.6 mJ irradiation at the same wavelength. The irradiance spot is centred at 2 mm horizontal and -4 mm vertical position. Each grey scale step is 0.4 %.

Figure 5. Long-term stability of the different types of detector used in the comparison: Relative change in responsivity between initial (Oct 06) and final (Aug 07) calibration at PTB (circles: SUV 100, squares: SXUV-100, diamonds: AXUV-100G). For SXUV and AXUV photodiodes, the open symbols represent the data from reference detectors stored at PTB. Positive values correspond to an increase in responsivity. The SXUV "A" diode is not shown here since it diverges more than 10 % and would be out-of-scale.
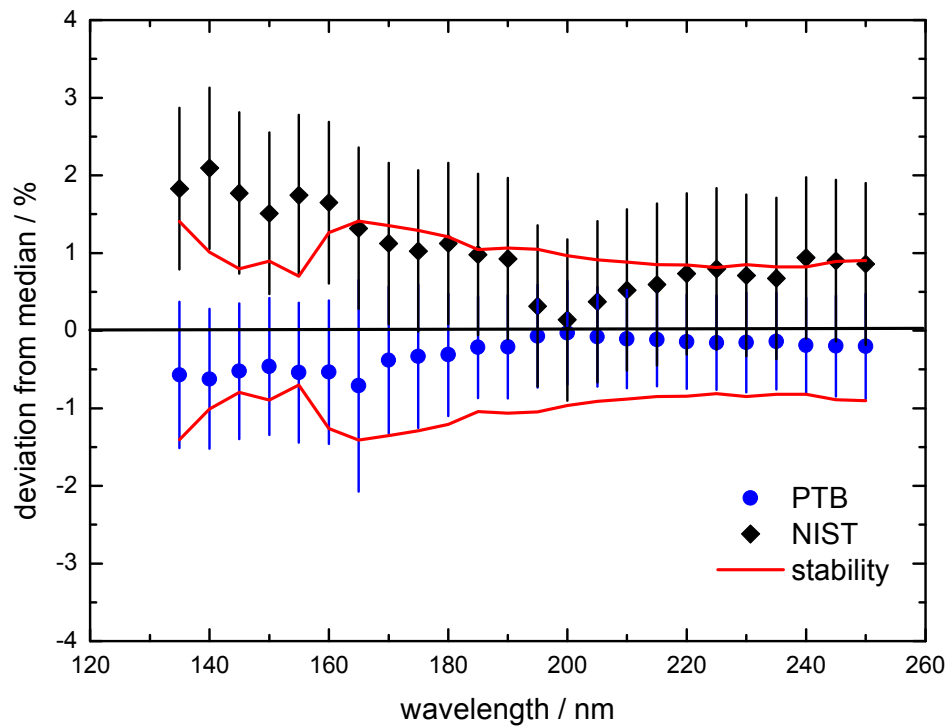
Figure 6. Relative deviation of the PTB and the NIST calibrated spectral responsivities to the

weighted median of both values, averaged over all four detectors in comparison. The solid lines

indicate the range of detector stability (k=2) deduced from the initial and the final PTB measurements.

References

[1] Scholze F, Vest R, Saito T 2010 *Metrologia* **47** 02001

[2] Shaw P-S, Larason T C, Gupta R, Brown S W, Vest R E, Lykke K R 2001 *Rev. Sci. Instrum.* **72** 2242–2247

[3] Gottwald A, Kroth U, Krumrey M, Richter M, Scholze F, Ulm G 2006 *Metrologia* **43** S125–S129

[4] Arp U, Farrell A P, Furst M L, Grantham S, Hagley E, Kaplan S G, Shaw P-S, Tarrio C S, Vest R E 2003 *Synchrotron Radiat. News* **16**(5) 30-36

[5] Ulm G, Radiometry with synchrotron radiation 2003 *Metrologia* **40** S101–S106

[6] Beckhoff B, Gottwald A, Klein R, Krumrey M, Müller R, Richter M, Scholze F, Thornagel R, Ulm G 2009 *Phys. Status Solidi B* **246** 1415-1434

[7] Richter M, Hollandt J, Kroth U, Paustian W, Rabus H, Thornagel R, Ulm G 2001 *Nucl. Instr. and Meth.* **A 467–468** 605–608

[8] Gerlach M, Krumrey M, Cibik L, Müller P, Rabus H, Ulm G 2008 *Metrologia* **45** 577

[9] Rabus H, Persch V, Ulm G 1997 *Appl. Opt.* **36** 5421–5440

[10] Shaw P-S, Lykke K R, Gupta R, O'Brian T R, Arp U, White H H, Lucatorto T B, Dehmer J L, Parr A C 1998 *Metrologia* **35** 301–306

[11] Korde R, Prince C, Dunningham D, Vest R E, Gullikson E 2003 *Metrologia* **40** S145–S149

[12] Shaw P-S, Gupta R, Lykke K R 2005 *Appl. Opt.* **44** 197–207

[13] Richter M, Kroth U, Gottwald A, Gerth C, Tiedtke K, Saito T, Tassy I, Vogler K 2002 *Appl. Opt.* **41** 7167–7172

[14]. Scholze F, Klein R, Bock T 2003 *Appl. Opt.* **42** 5621-5626

[15] Solt K, Melchior H, Kroth U, Kuschnerus P, Persch V, Rabus H, Richter M, Ulm G 1996 *Appl. Phys. Lett.* **69** 3662–3664

[16] Kjornrattanawanich B, Korde R, Boyer C N, Holland GE, Seely J F 2006 IEEE Transactions on

   Electron. Devices **53** 218-223